A regime diagram of a slurry F-layer

Jenny Wong (Institut de Physique du Globe de Paris)

Chris Davies (University of Leeds)

Chris Jones (University of Leeds)

Engineering and Physical Sciences Research Council

Natural Environment Research Council

IPGP Institut de Physique du Globe de Paris | Université de Paris

UNIVERSITY OF LEEDS

AGU 100 ADVANCING EARTH AND SPACE SCIENCE

Stratified layers in the core?

- Classic picture: vigorous convection ⇒ well-mixed, liquid, metallic alloy
- Adiabatically stratified and homogeneous
- Thin boundary layers
- Recent picture: stably stratified layers exist beneath the CMB and above ICB
- How did they develop? How are they sustained? How do they impact core dynamics?

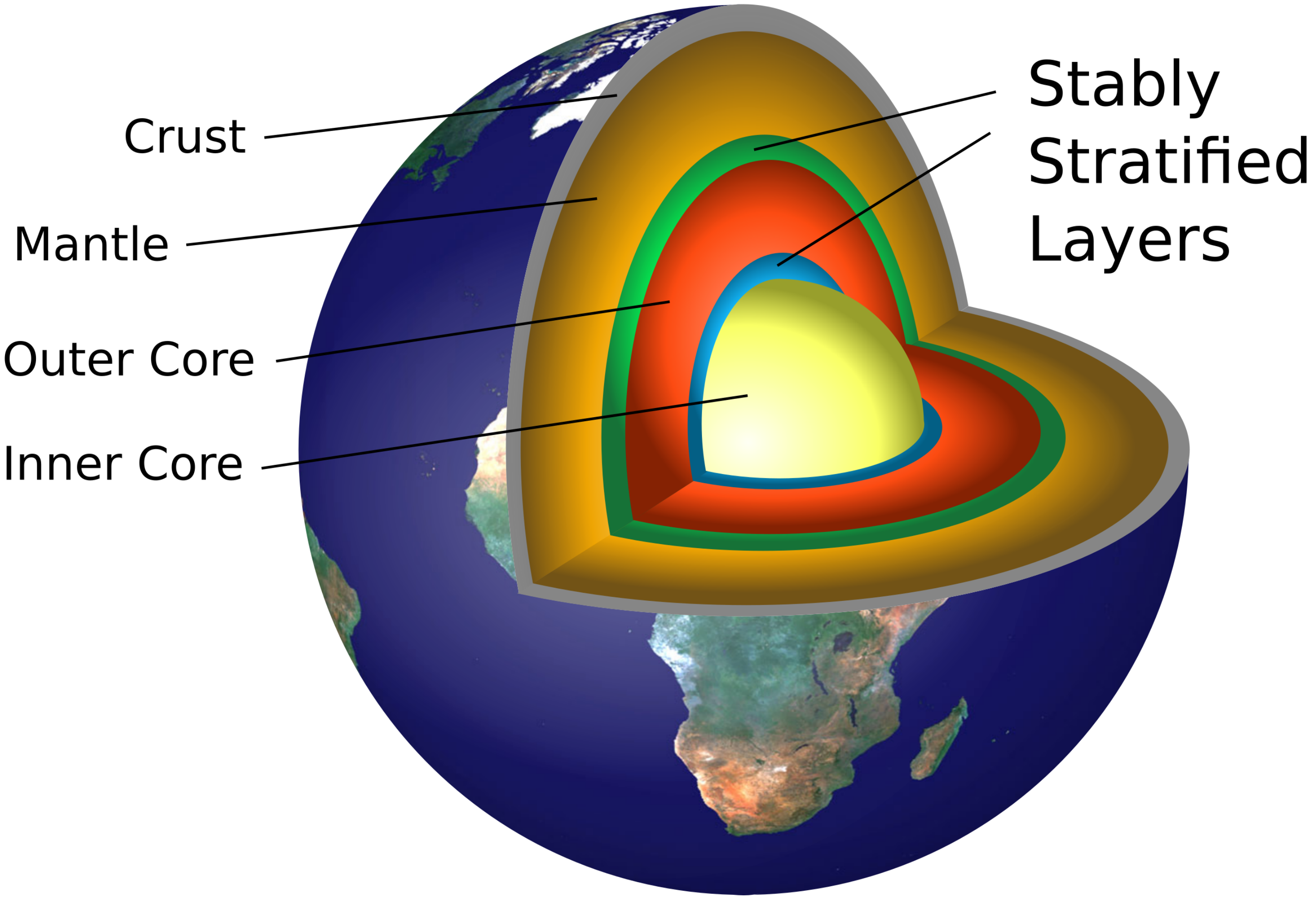

Hardy and Wong (2019)

Seismic observations of the F-layer

- PREM assumes that the liquid core is adiabatically stratified
- Slower than expected P wave speed observed
- P wave speed is inversely proportional to density

Ohtaki et al. (2018)

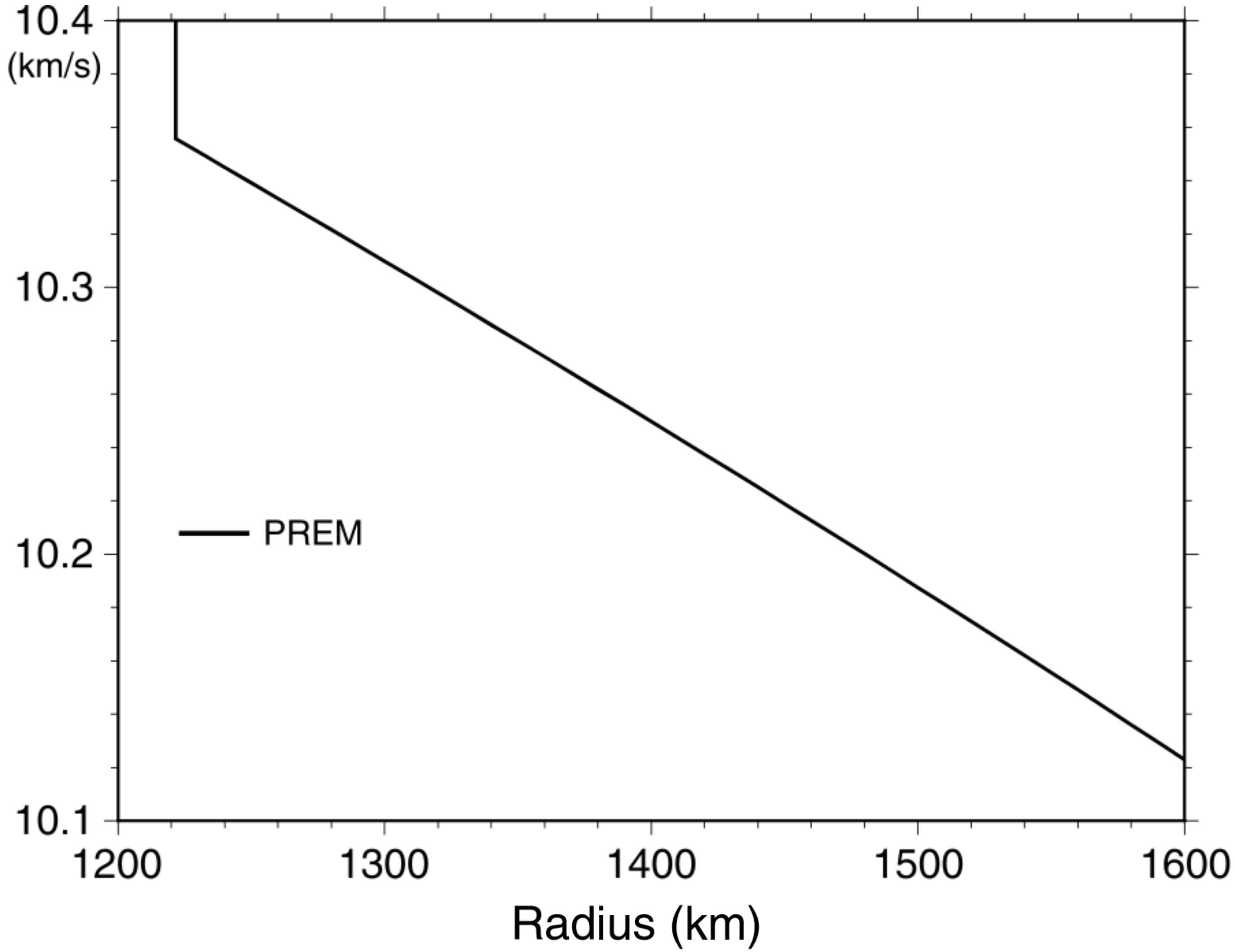

Seismic observations of the F-layer

- PREM assumes that the liquid core is adiabatically stratified
- Slower than expected P wave speed observed
- P wave speed is inversely proportional to density

Ohtaki et al. (2018)

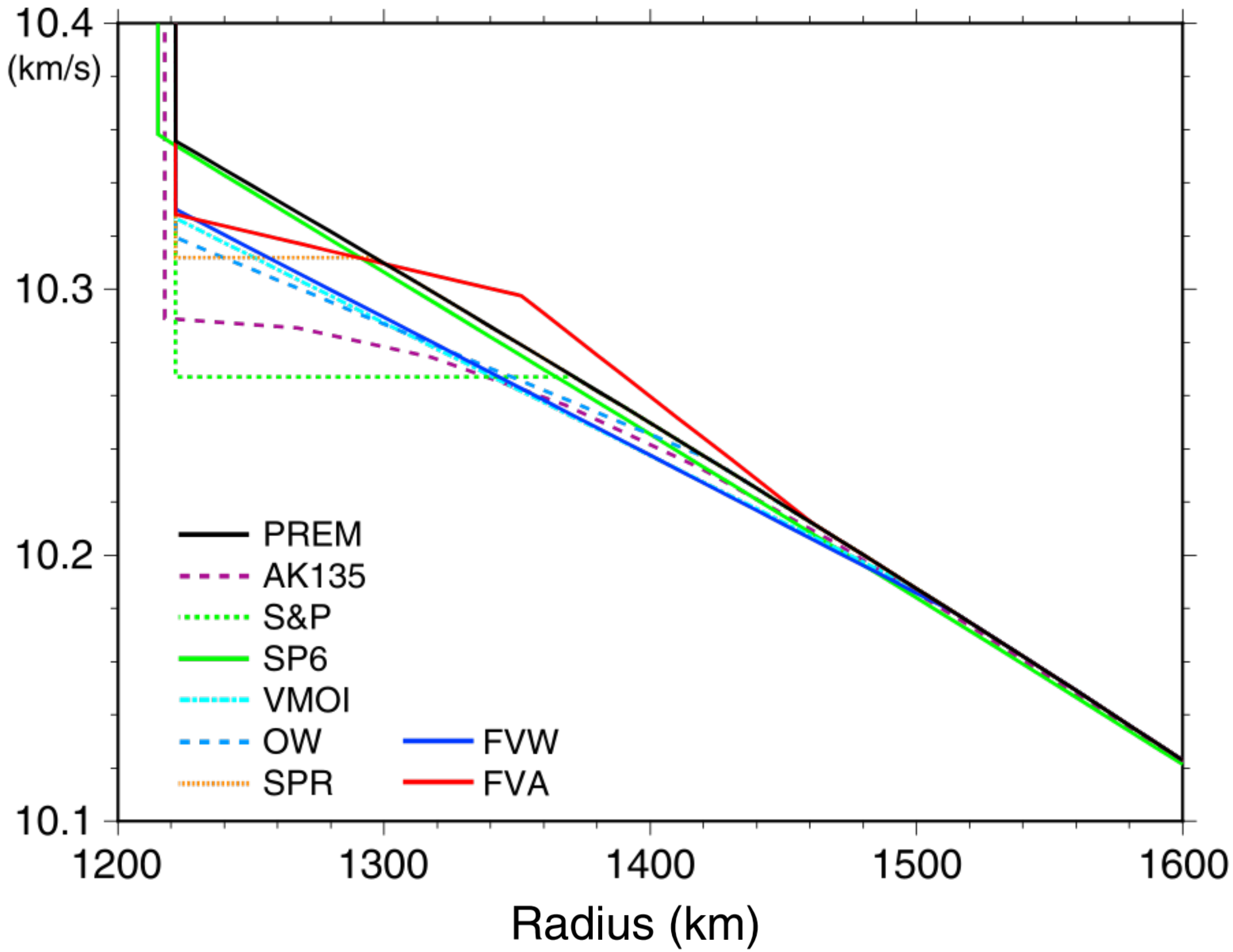

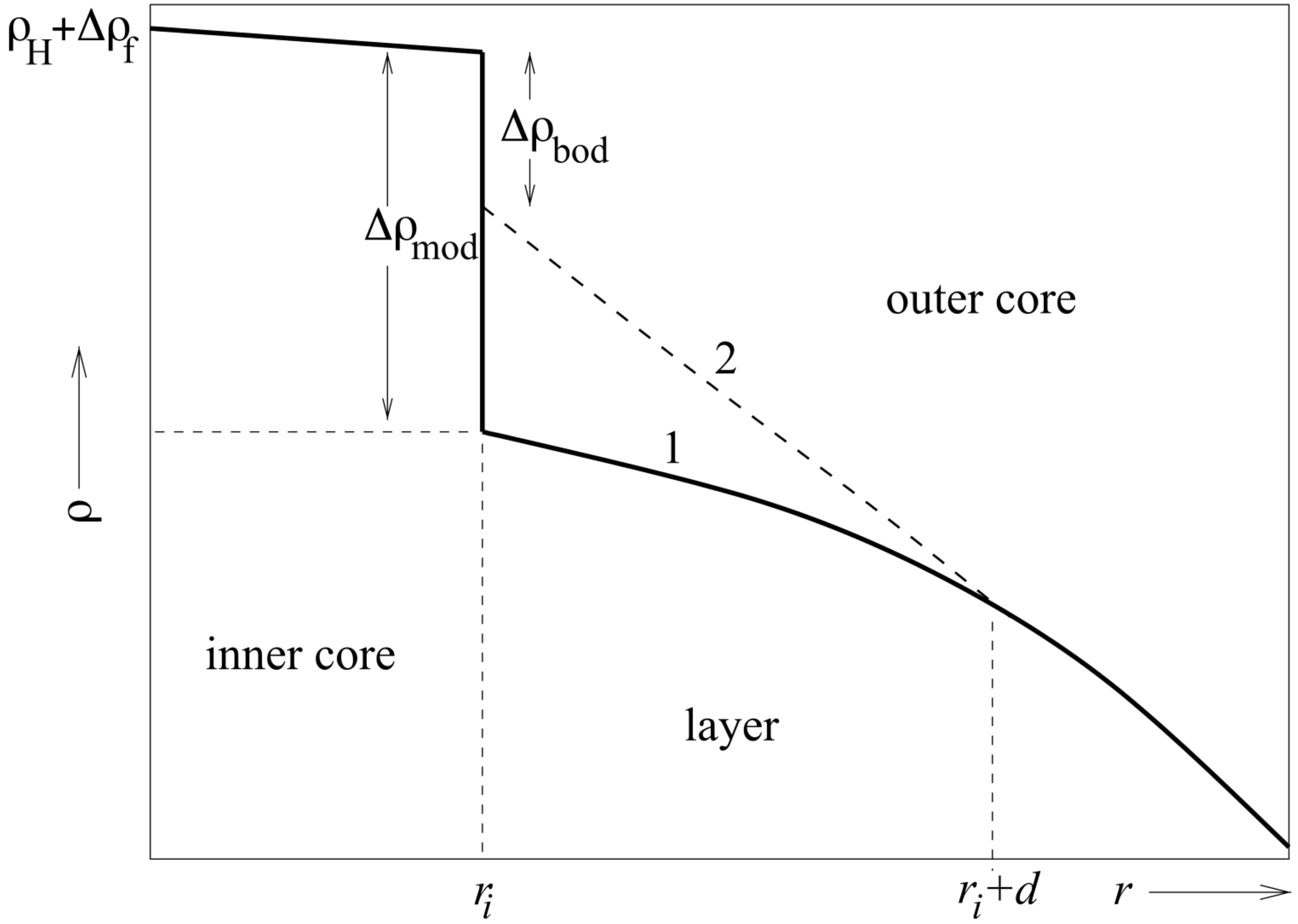

Gubbins et al. (2008)

Seismic density structure

- Discrepancy between $\Delta\rho_{mod}$ and $\Delta\rho_{bod}$
- This infers a stably stratified layer exists
- How can light elements pass through the layer and out into the bulk of the core?
- Layer is not a thermal boundary layer

Possible scenarios

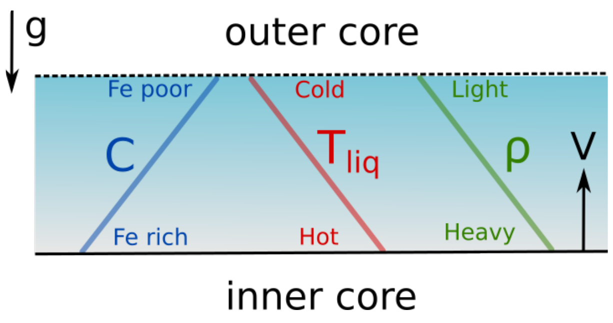

Thermochemical layer on the liquidus

(Gubbins et al. 2008)

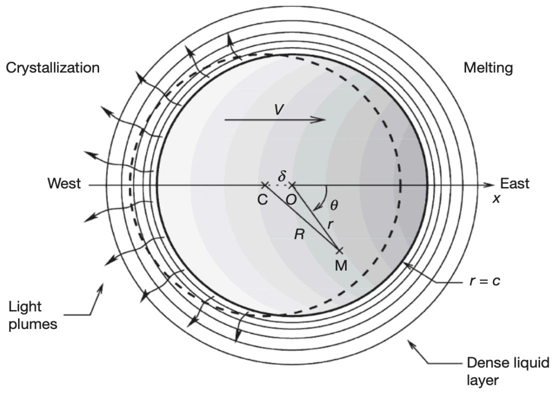

Convective translation

(Alboussière et al. 2010)

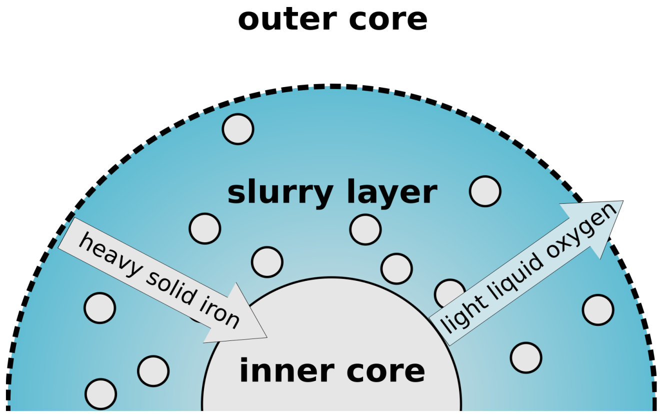

Slurry layer

(Wong et al. 2018, Loper and Roberts 1977)

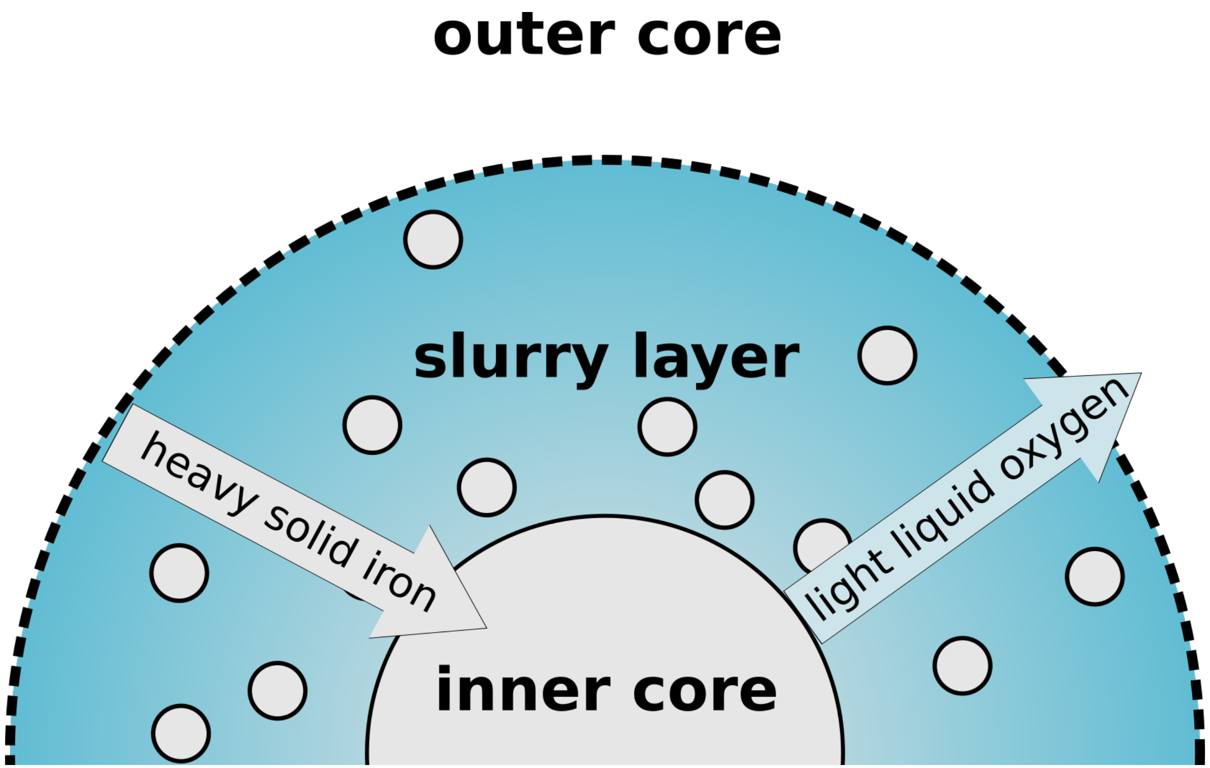

Slurry (iron snow) layer

- Two component (iron and oxygen), two phase (solid and liquid) system
- Formation and transport of solid phase provides a way for light element to cross a stably stratified layer
- Solid fraction is small

For full details see: Wong et al. (2018) https://doi.org/10.1093/gji/ggy245

Dimensionless parameters:

$$\text{Péclet} \sim Q_i \qquad \text{Stefan} \sim \frac{Q_{sl}}{Q_i} \qquad \text{Lewis} \sim k$$

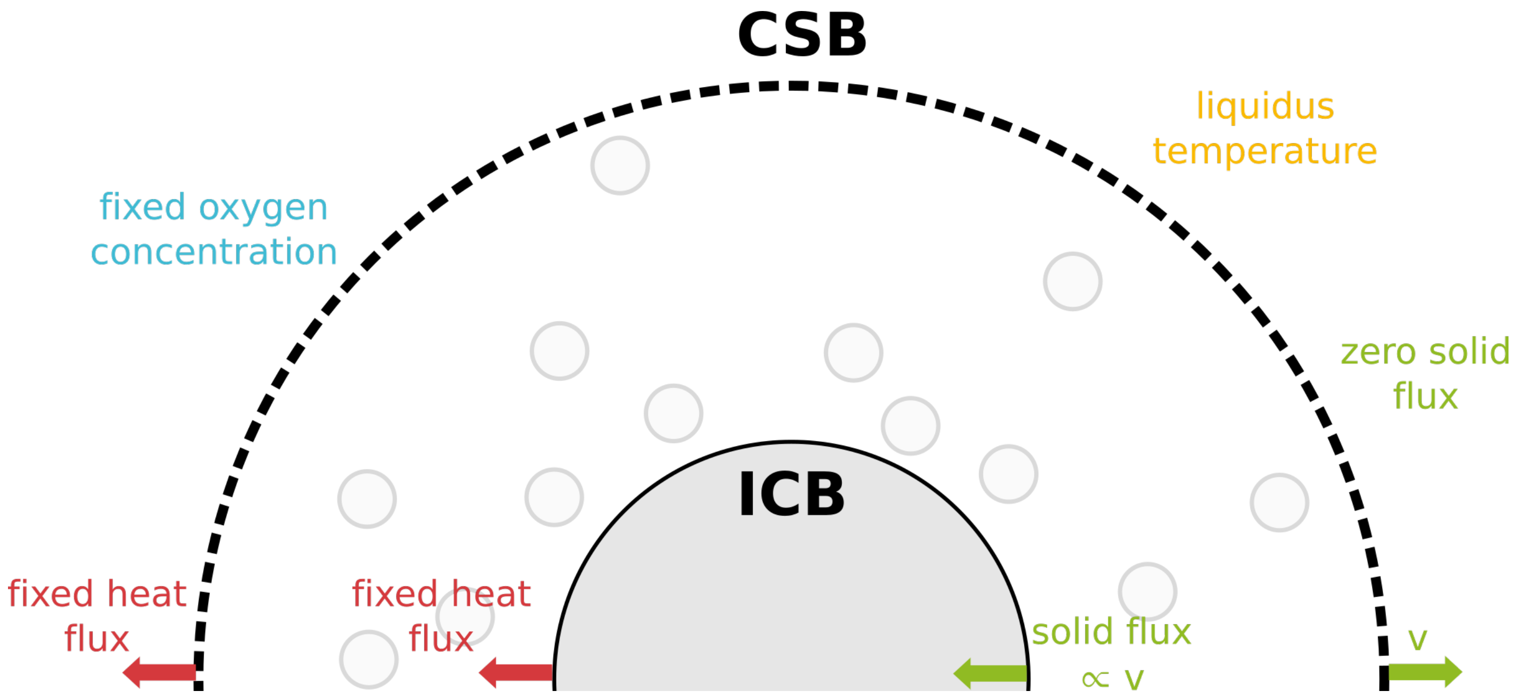

Slurry (iron snow) layer

- Governing equations:
  - Liquidus
  - Conservation of oxygen
  - Conservation of energy
- Reference frame of fixed layer thickness moving at IC growth rate
- Static slurry, 1D and spherical geometry

Geophysical constraints

	$\Delta\rho_{mod}\ (kg\ m^{-3})$	$\Delta\rho_{bod}\ (kg\ m^{-3})$
Maximum	1000 (Masters and Gubbins 2003)	1100 (Tkalčić et al. 2009)
Minimum	600 (PREM)	520 ± 240 (Koper and Dombrovskya 2005)

- Seismic density jump across the layer

$$\Delta\rho \equiv \rho_{sl}(r_i) - \rho_{PREM}(r_{sl}) \equiv \Delta\rho_{mod} - \Delta\rho_{bod} < 720\ kg\ m^{-3}$$

- CMB heat flow *(Lay et al. 2008)*

$$5 < Q^c < 15\ TW$$

- ICB heat flow *(Pozzo et al. 2014)*

$$Q^i < 2\ TW$$

Results

- Temperature gradient is "locked" to the oxygen gradient via the liquidus
- Solid flux is negative down towards ICB

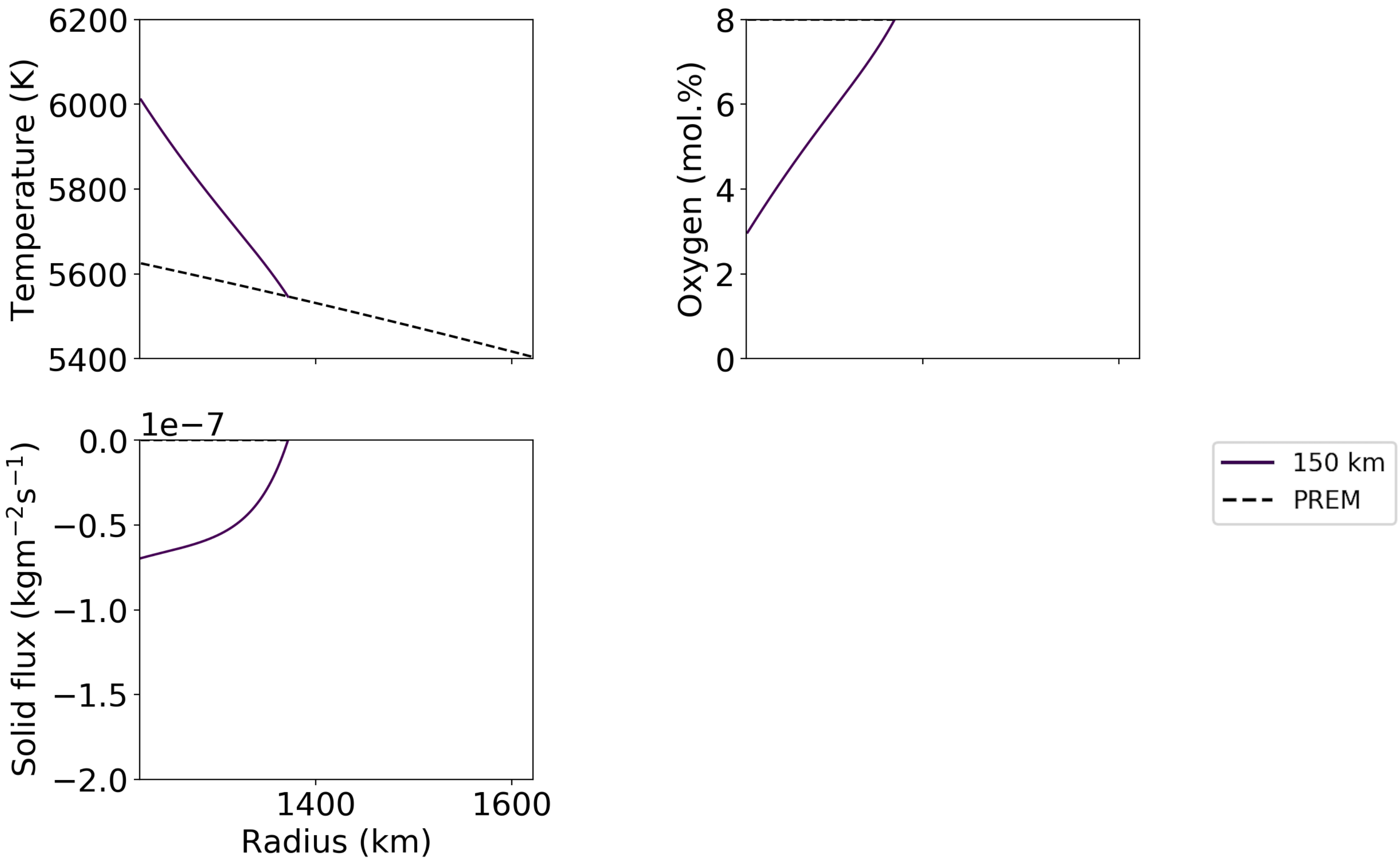

Results

- Temperature, oxygen and solid fraction contribute to density anomaly
- Solid fraction obtained from solid flux by assuming Stokes' flow

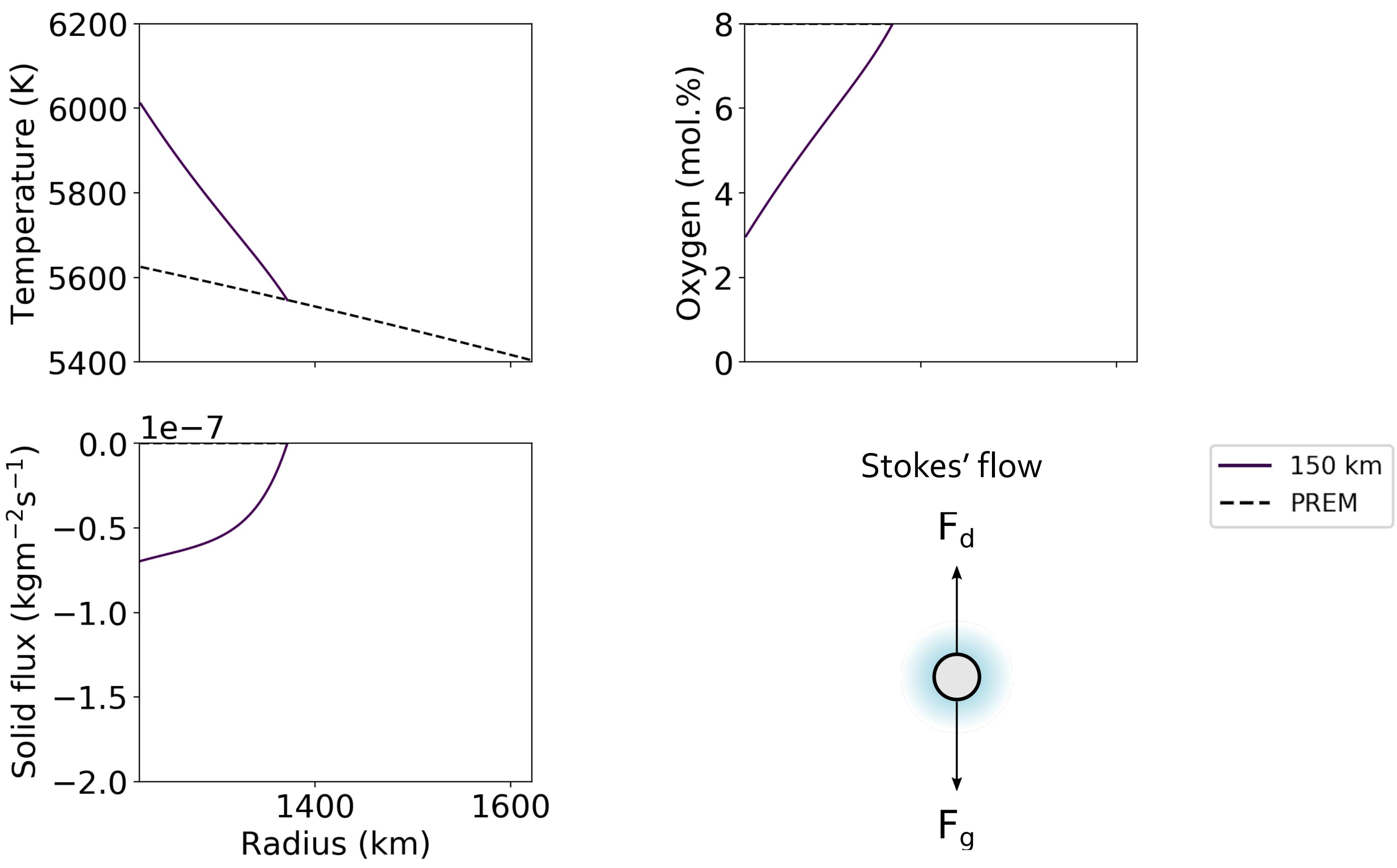

Results

- Slurry density and density gradient exceeds PREM ⇒ a stably stratified layer

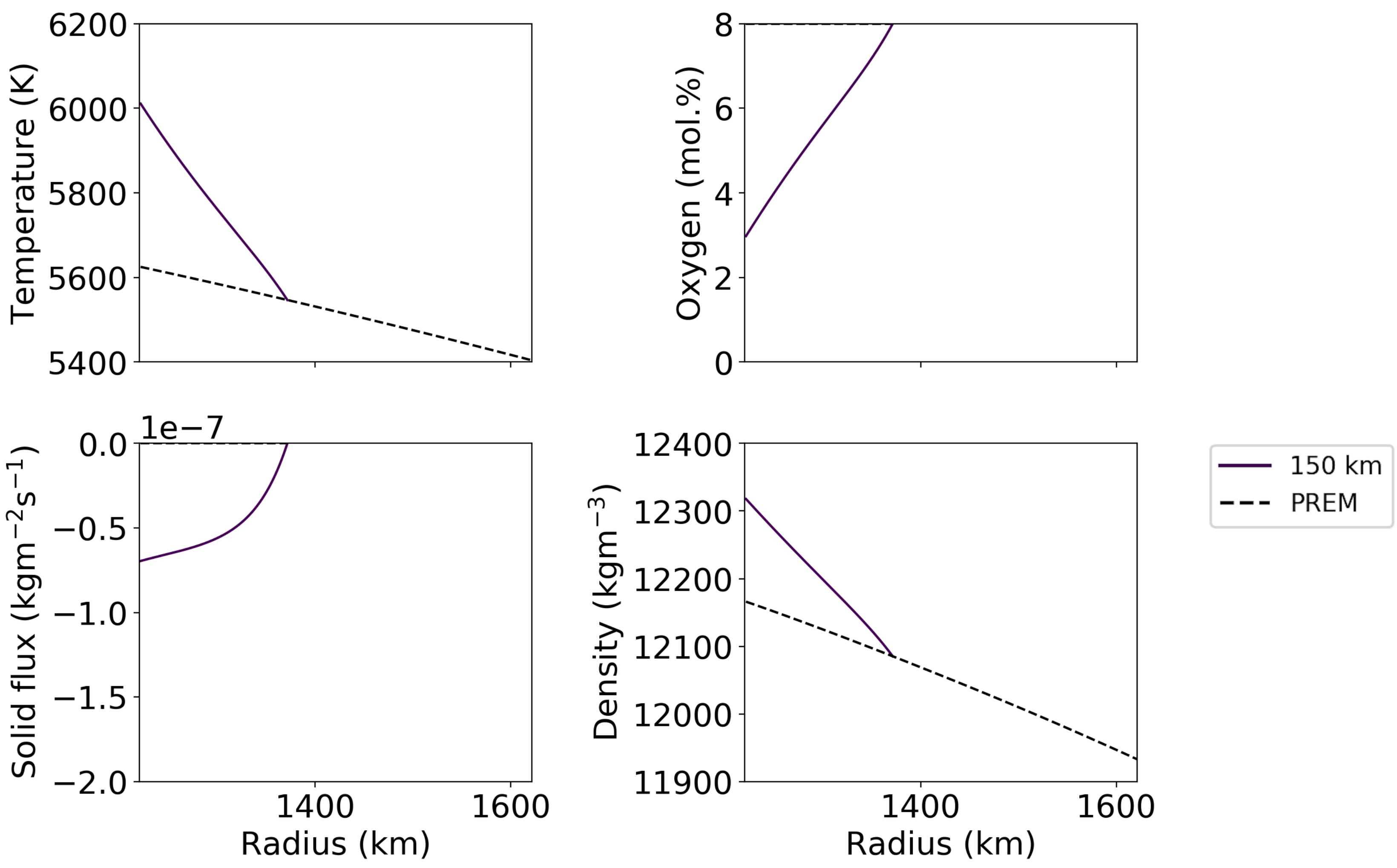

Results

- Increasing layer thickness increases the density jump across the layer
- Layer becomes destabilised at mid-depths

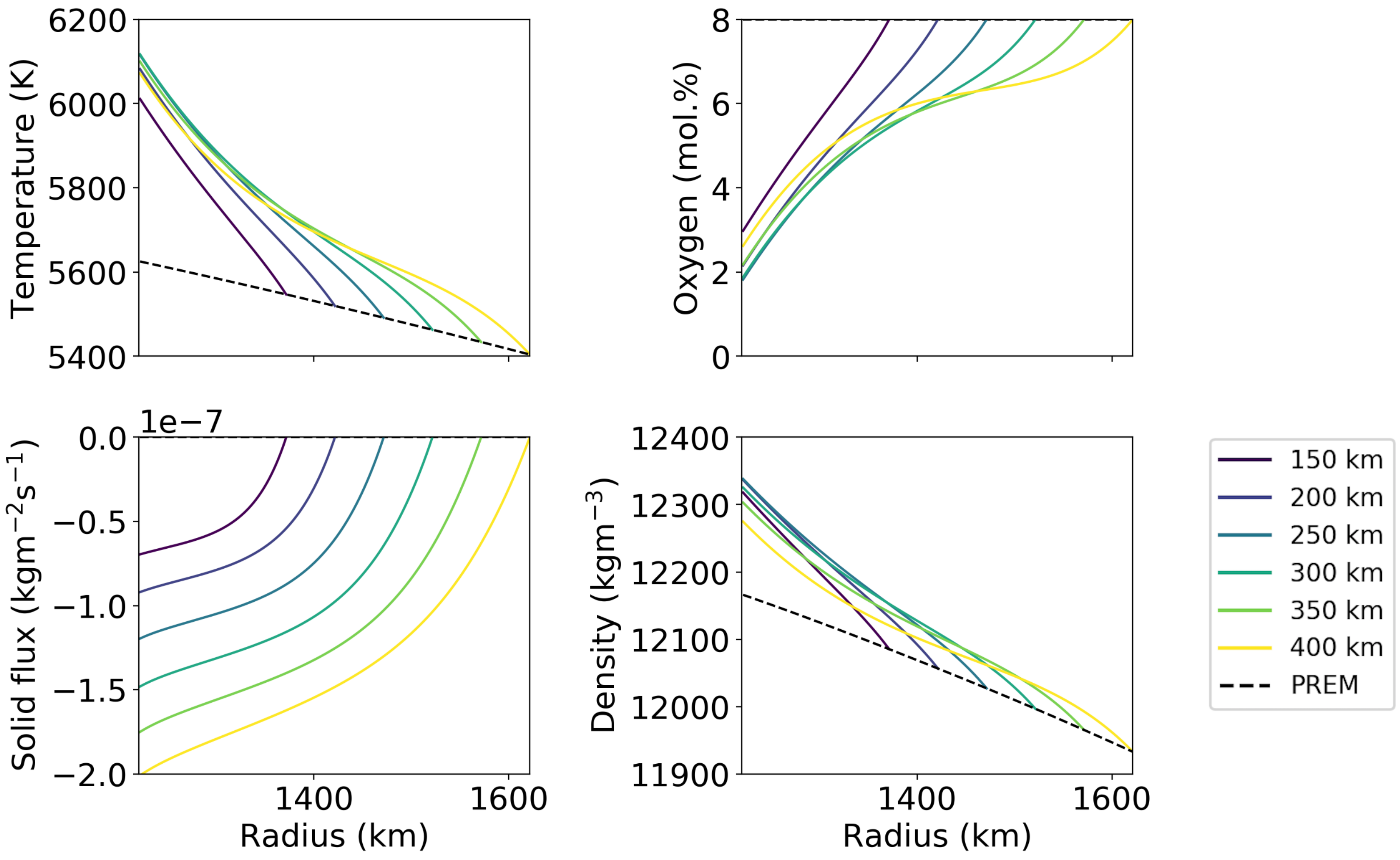

Regime diagram

Layer thickness = 150 km

STABLE: slurry density and density gradient exceed PREM

PARTIALLY STABLE: slurry density and density gradient exceeds PREM over 100+ km

UNSTABLE: slurry density or density gradient is below PREM

NO SLURRY

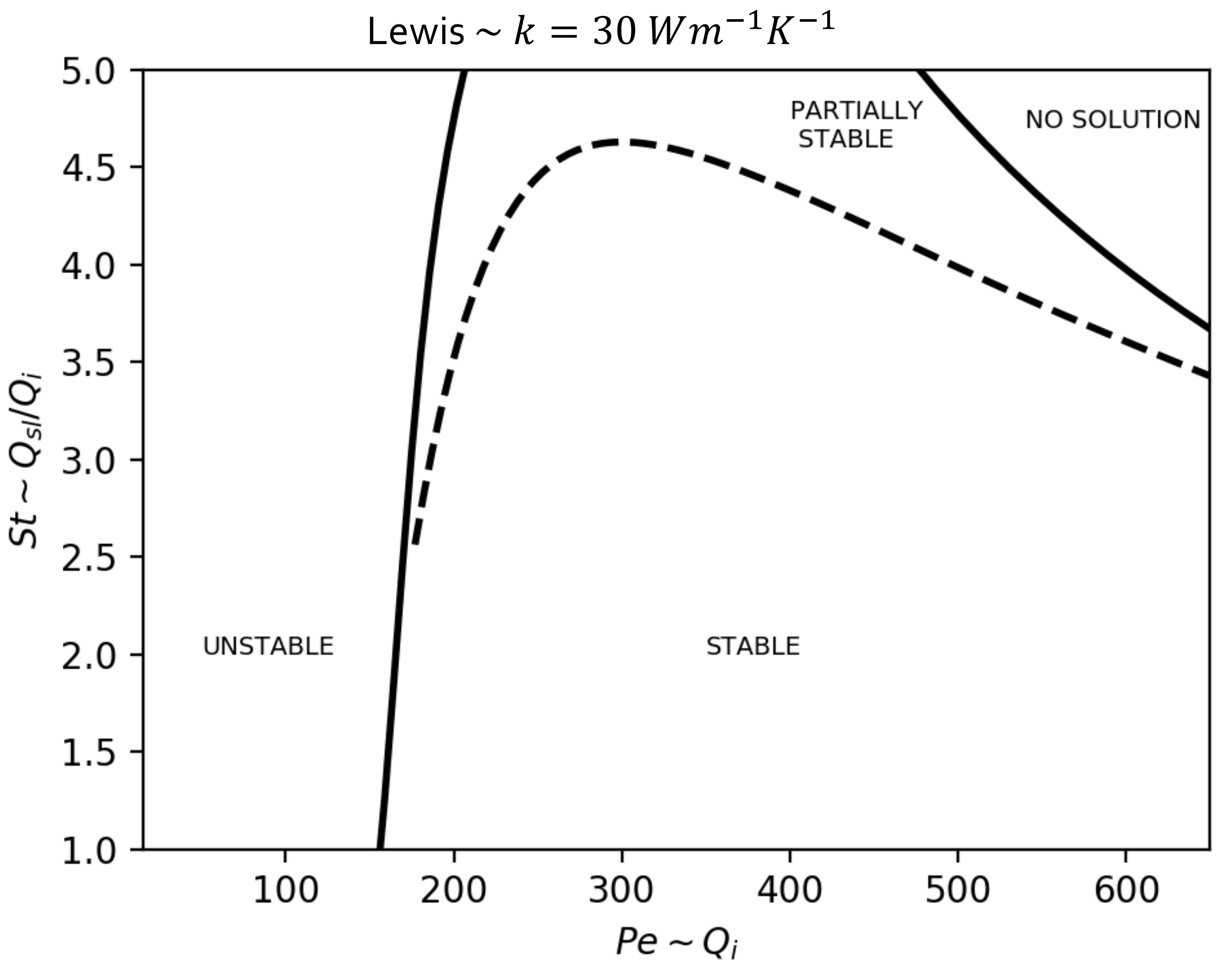

Regime diagram

The greatest density jumps are found in the high Peclet, high Stefan number region.

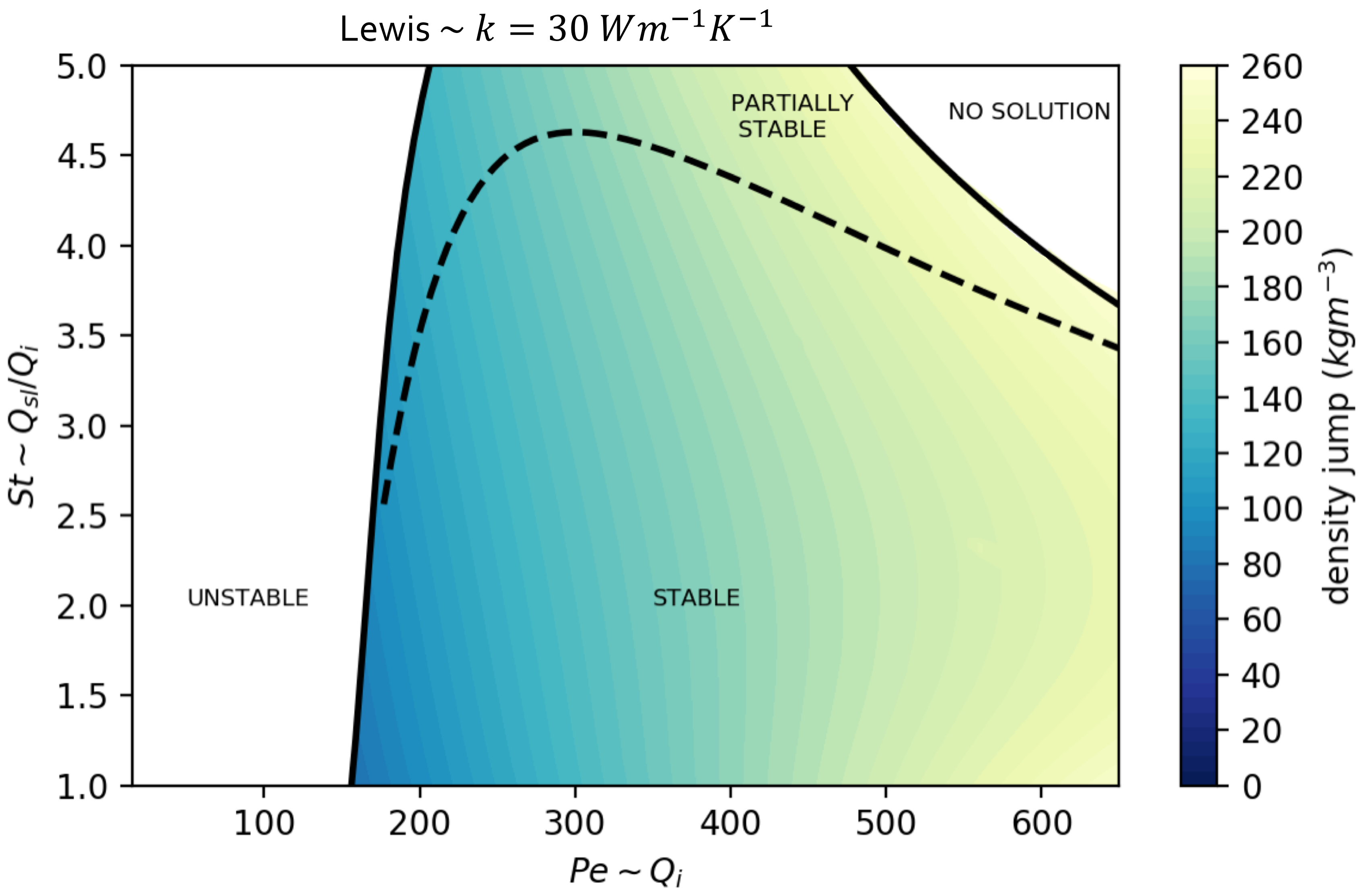

Regime diagram

The greatest density jumps are found in the high Peclet, high Stefan number region.

Increasing layer thickness is in high Peclet, low Stefan number region.

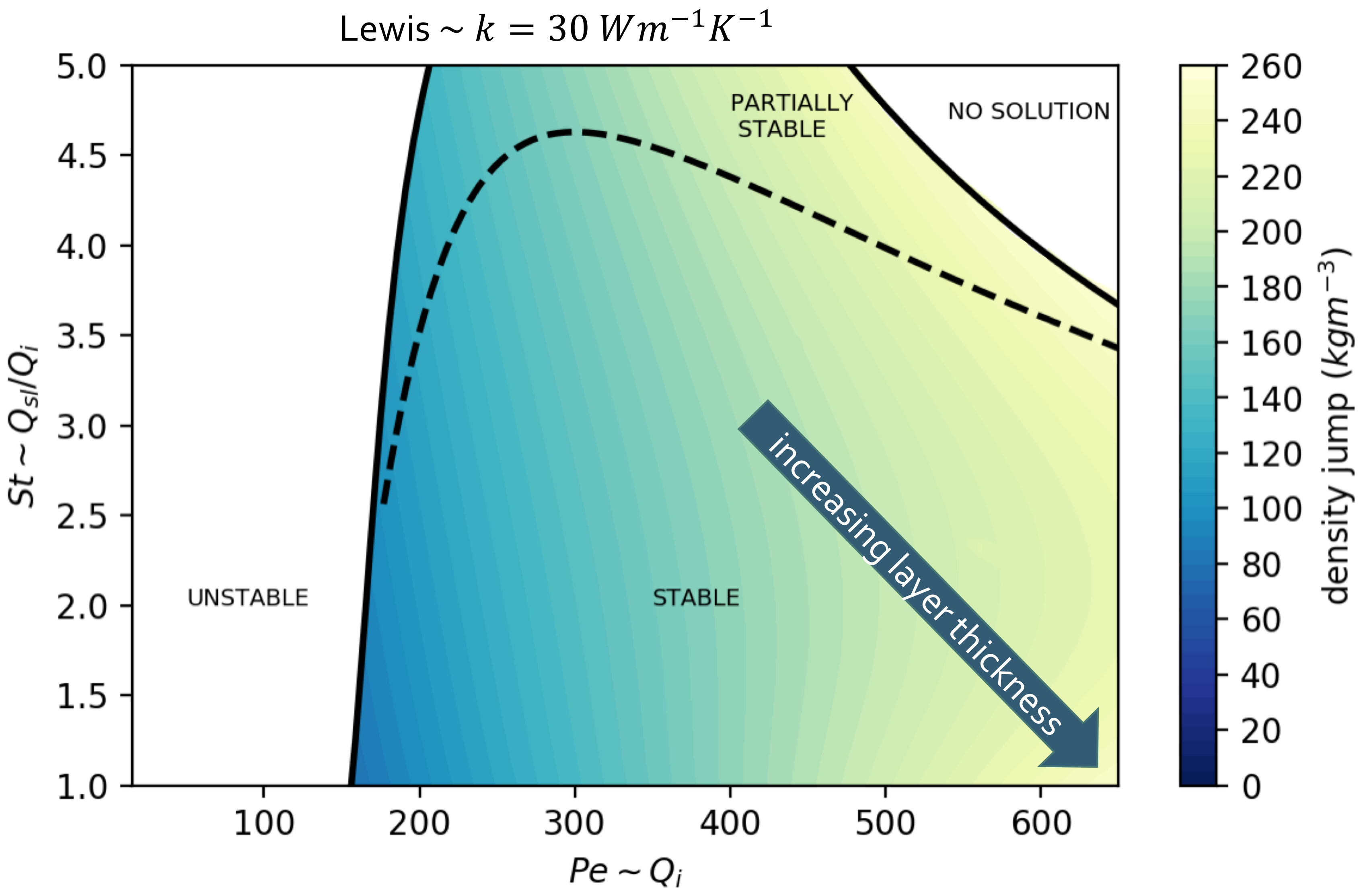

Regime diagram

CMB heat flow is proportional to the imposed CSB heat flow.

Within constraint of
$5 < Q_c < 15\,TW$.

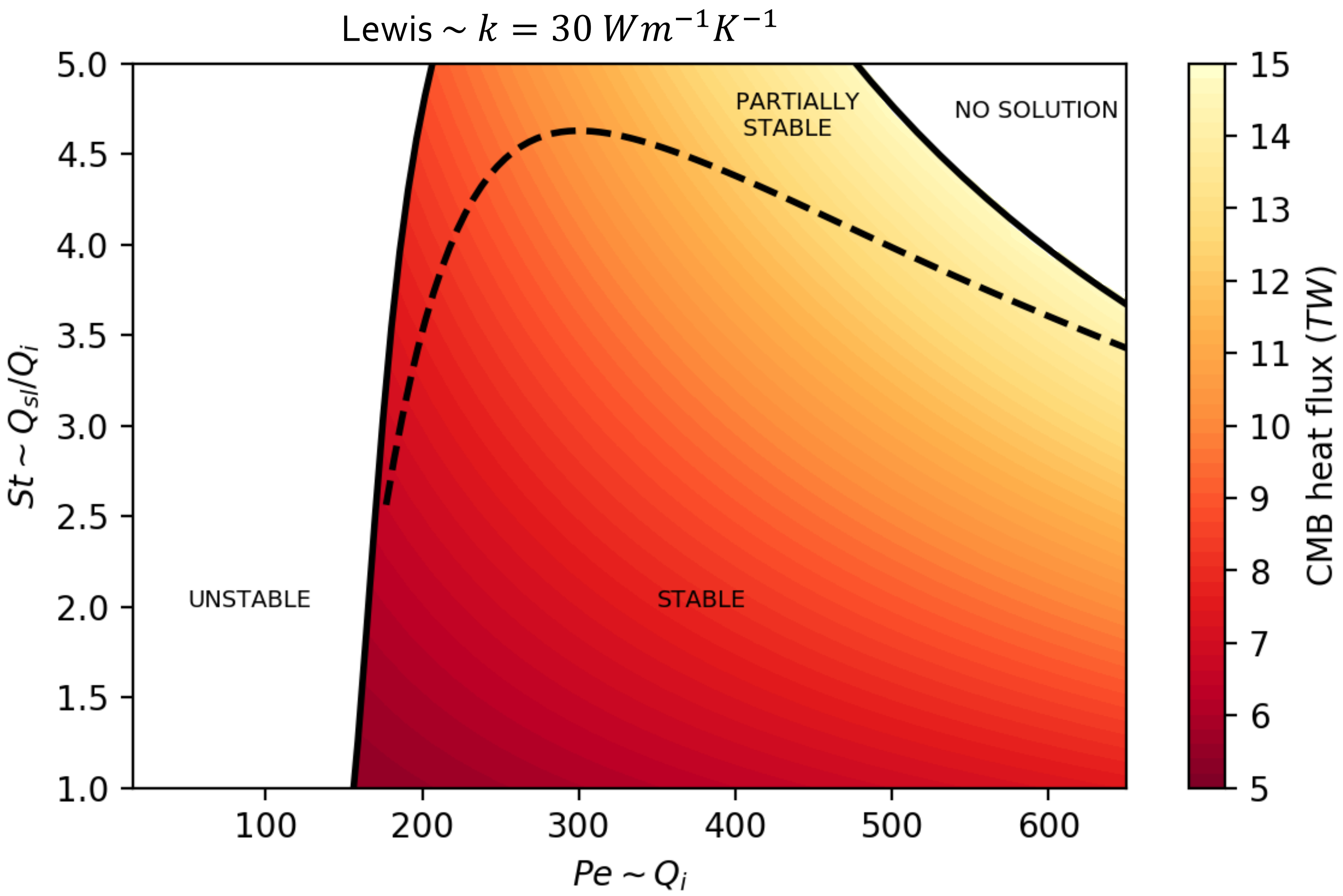

Low thermal conductivity

Lewis $\sim k = 30\ Wm^{-1}K^{-1}$

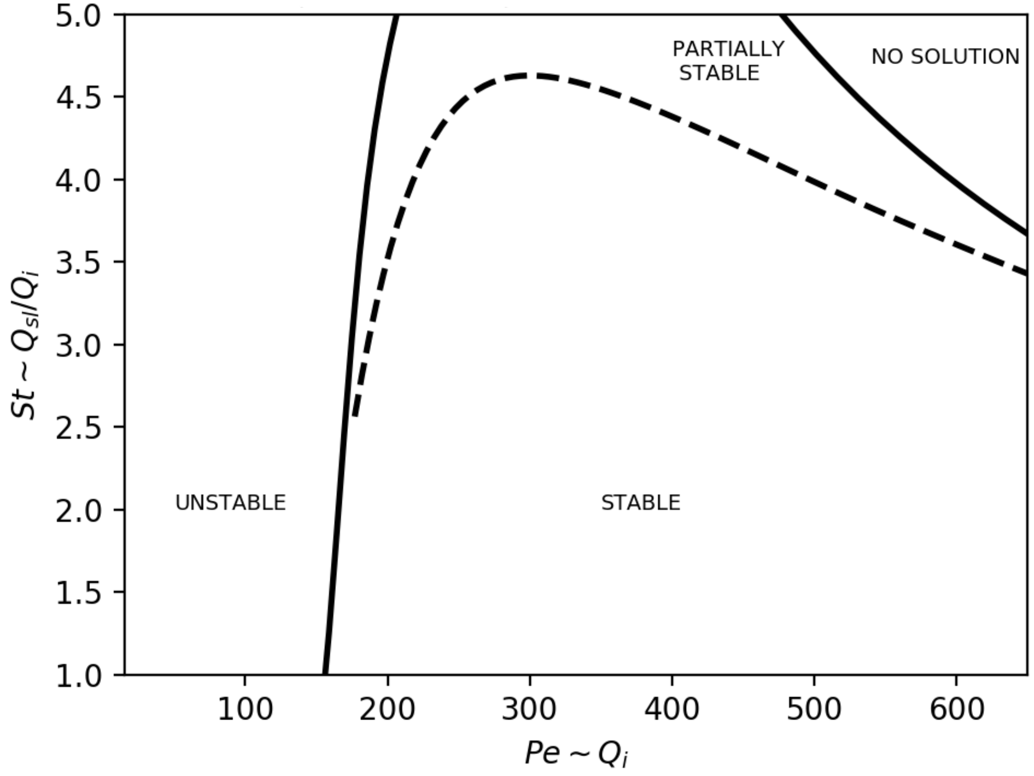

High thermal conductivity

Lewis $\sim k = 100\ Wm^{-1}K^{-1}$

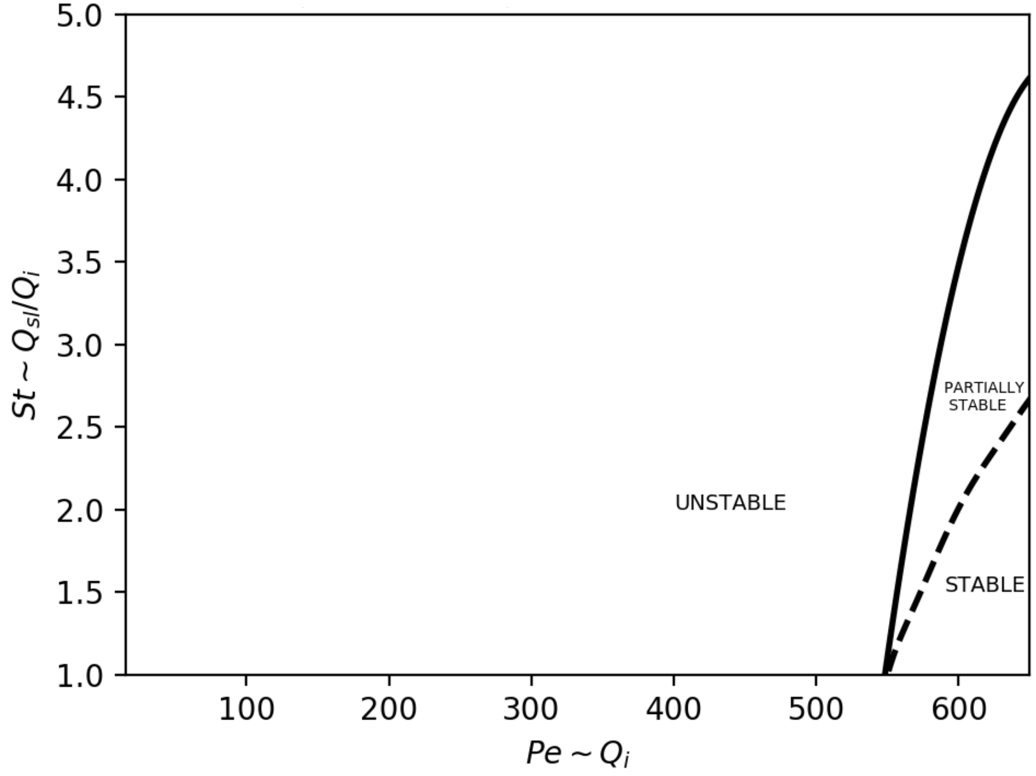

Stably stratified layers found when ICB heat flux is closer to 2 TW.

Low thermal conductivity

High thermal conductivity

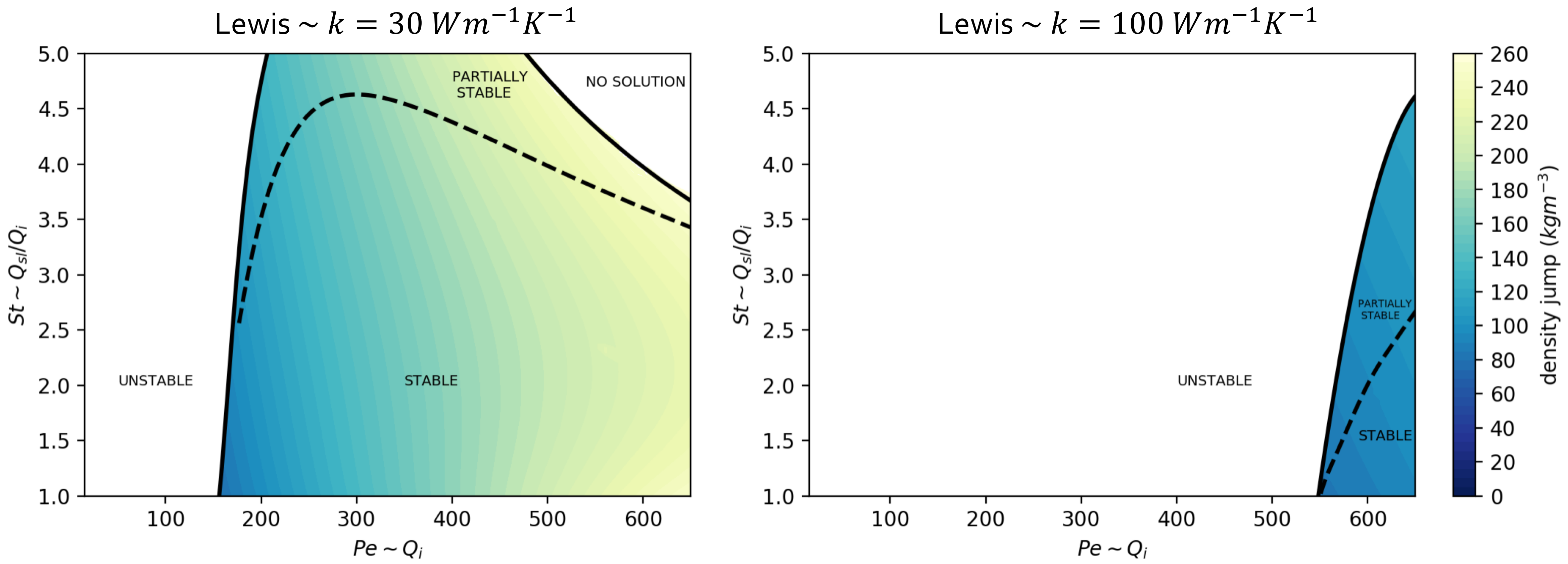

The density jump is smaller and the greatest values are also found at higher Stefan number.

Taking $\Delta\rho_{bod} = \Delta\rho_{mod} - \Delta\rho_{slurry}$ then $350 < \Delta\rho_{bod} < 750\ kg\ m^{-3}$ for low thermal conductivity,

$500 < \Delta\rho_{bod} < 900\ kg\ m^{-3}$ for high thermal conductivity.

Summary

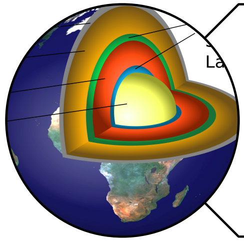

Stratified layers in the core?

Consensus on slowdown in P-wave speed at the base of the core.

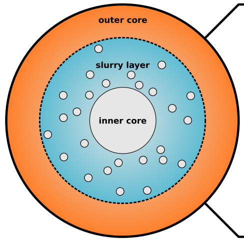

Slurry (iron snow) layer

A slurry provides a thermodynamic explanation of the stratified F-layer.

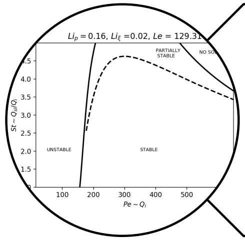

Regime diagram

High density jumps for low thermal conductivity, high ICB and CSB heat fluxes.

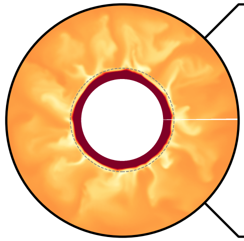

Future work

How does a stratified F-layer impact core dynamics and the dynamo?

Model assumptions

Fast melting

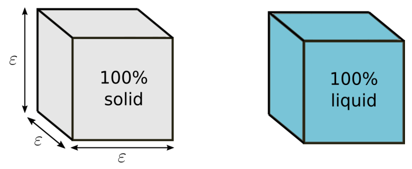

Binary alloy

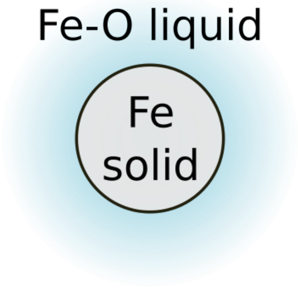

Isothermal inner core

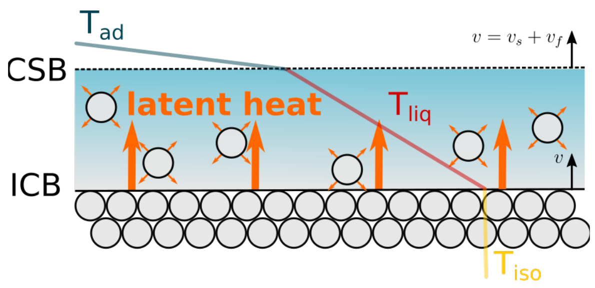

Stokes' flow

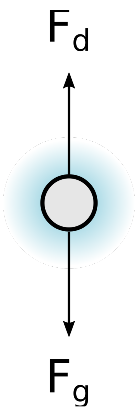

Model details

Alfé et al. (2002)

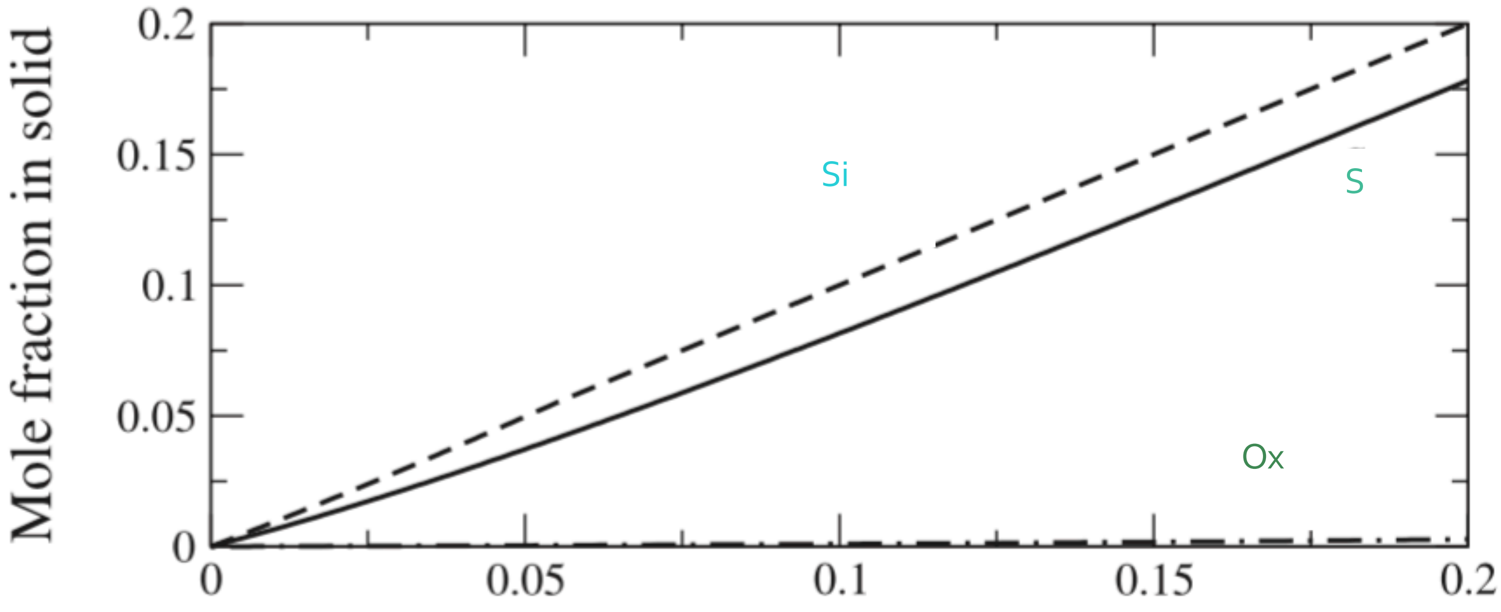

- Oxygen partitions entirely into the liquid

Dimensionless equations

$$\frac{\partial \theta}{\partial r} = -Li_p g \rho \theta - Li_\xi St^* \theta^2 \frac{\partial \Xi}{\partial r},$$

$$\Xi \frac{\partial j}{\partial r} = \frac{1}{r^2} \frac{\partial}{\partial r} \left(\frac{Li_p}{Li_\xi St^* Pe^*} \frac{g \rho r^2}{\theta} \exp\left[\frac{F\left(r_{sl} r - r_i\right)}{d} \right] \right) - \frac{v_s}{v_f} \frac{\partial \Xi}{\partial r} - \left(\frac{\partial \Xi}{\partial r} + \frac{2}{r} \Xi \right) j$$

$$\frac{\partial^2 \theta}{\partial r^2} = -\frac{Pe^*}{St^* Le^*} \left(\frac{\partial j}{\partial r} + \frac{2}{r} j \right) - \left(\frac{v_s}{v_f} \frac{Pe^*}{Le^*} + \frac{2}{r} \right) \frac{\partial \theta}{\partial r}$$

Dimensionless parameters

$$Li_p \equiv \frac{\Delta V_{Fe}^{s,l} g_{sl} \rho_{sl} r_{sl}}{L},$$

$$Li_\xi \equiv \frac{1000 R \xi_O}{a_O c_p},$$

$$Pe^* \equiv \frac{v_f r_{sl} \Delta V_{Fe}^{s,l}}{D_O \Delta V_{Fe,O}^{s,l}}$$

$$St^* \equiv \frac{Q^{sl}}{4 \pi r_{sl}^2 \rho_{Fe}^l v_f L},$$

$$Le^* \equiv \frac{k \Delta V_{Fe}^{s,l}}{\rho_{Fe}^l c_p D_O \Delta V_{Fe,O}^{s,l}}.$$

Dimensionless boundary conditions

$$\theta(1) = \frac{T_l c_p}{St^* L},$$

$$\left. \frac{\partial \theta}{\partial \hat{r}} \right|_{\hat{r} = \frac{r_i}{r_{sl}}} = -\frac{Pe^* St^* \rho_{Fe}^s}{Le^* \rho_{Fe}^l},$$

$$\left. \frac{\partial \theta}{\partial \hat{r}} \right|_{\hat{r} = 1} = -\frac{Pe^*}{Le^*},$$

$$\Xi(1) = 1,$$

$$\hat{j}\left(\frac{r_i}{r_{sl}} \right) = -\frac{v_s \rho_{Fe}^s}{v_f \rho_{Fe}^l},$$

$$\hat{j}(1) = 0.$$

Results

- Increasing layer thickness increases the density jump across the layer
- Layer becomes destabilised at mid-depths

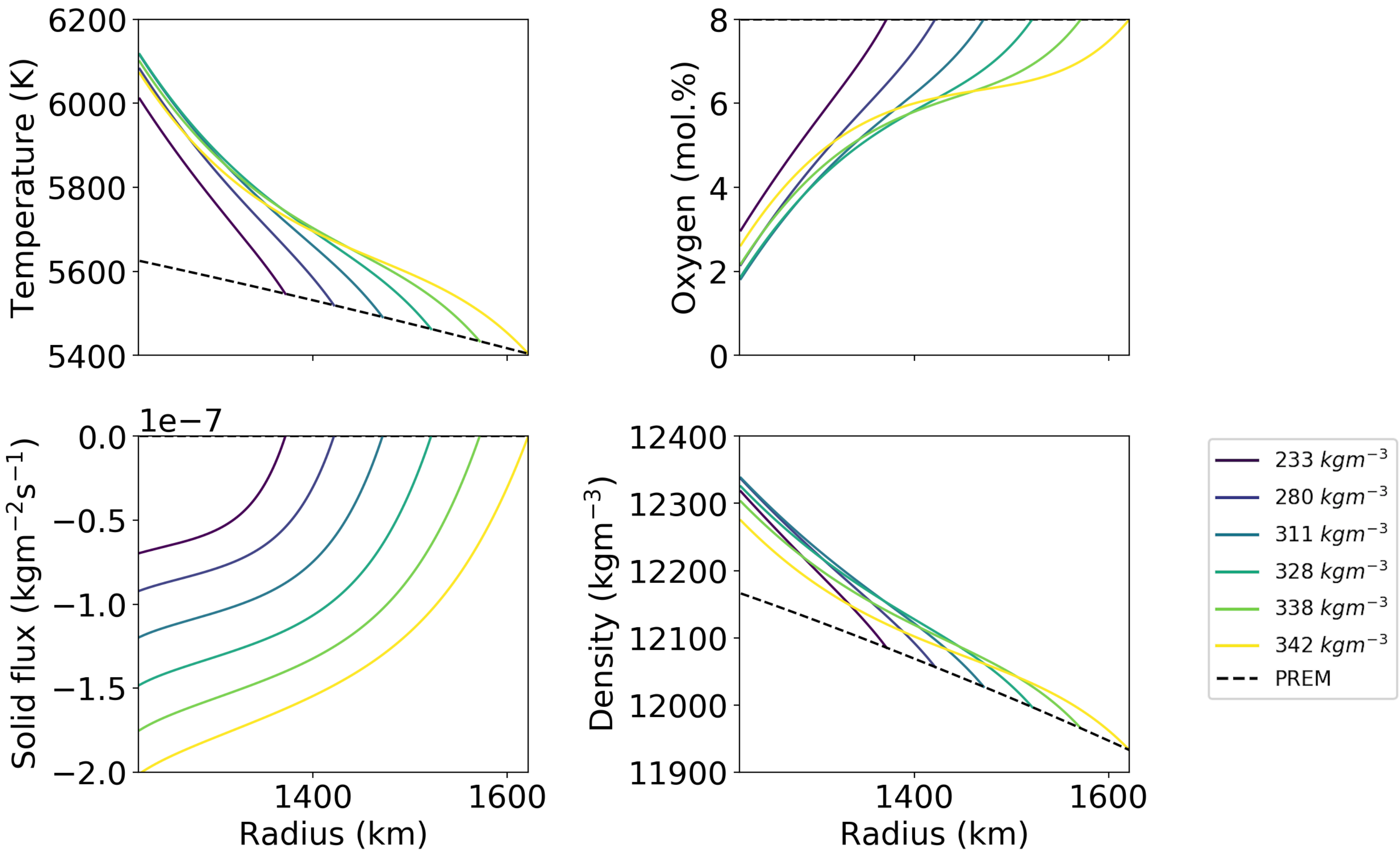

Parameter space

Dimensional		Dimensionless	
ICB heat flux	0.01 – 2 TW	Péclet	15 – 700
CSB heat flux	0.1 – 10 TW	Stefan	0.8 – 5.0
Thermal conductivity	30/100 $Wm^{-1} K^{-1}$	Lewis	129/431
Layer thickness	150 km	$Liquidus_{pressure}$	0.16
Bulk oxygen concentration	8 mol.%	$Liquidus_{composition}$	0.02

Low thermal conductivity

Lewis ~ $k = 30\ Wm^{-1}K^{-1}$

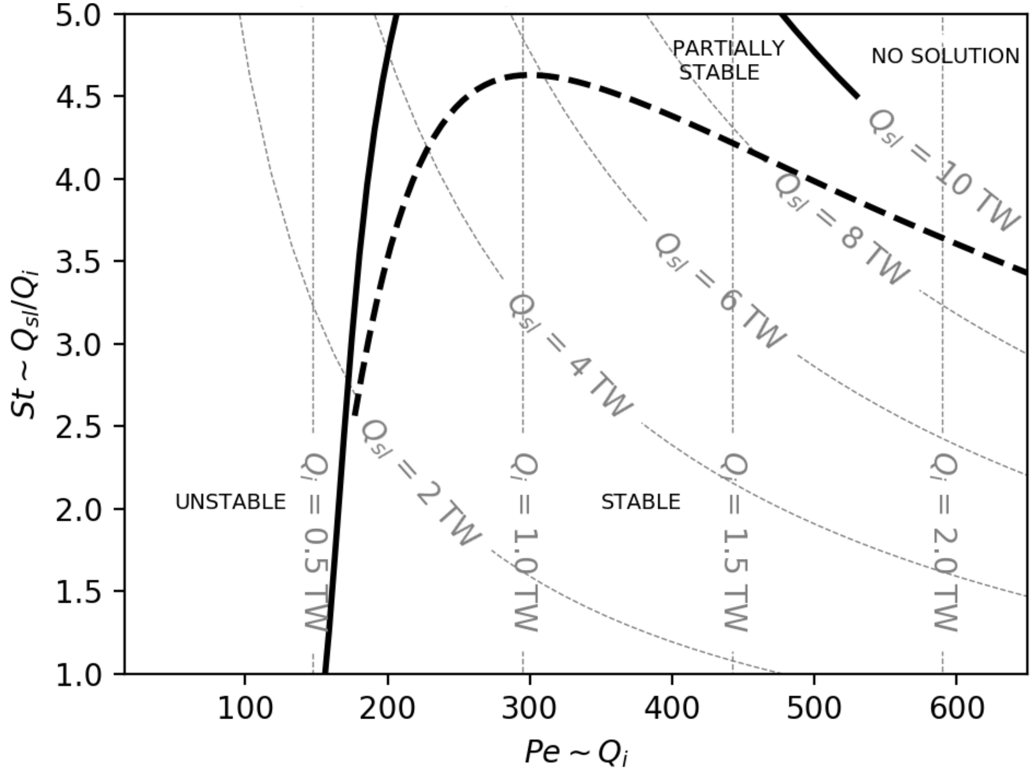

High thermal conductivity

Lewis ~ $k = 100\ Wm^{-1}K^{-1}$